Journal of Renewable Materials

Tech Science Press

DOI: 10.32604/jrm.2023.043659

ARTICLE

Chitosan/Sodium Alginate Multilayer pH-Sensitive Films Based on Layer-by-Layer Self-Assembly for Intelligent Packaging

Mingxuan He[1], Yahui Zheng[1], Jiaming Shen[1], Jiawei Shi[1], Yongzheng Zhang[1], Yinghong Xiao[2,*] and Jianfei Che[1,*]

[1]Key Laboratory of Soft Chemistry and Functional Materials, Nanjing University of Science and Technology, Nanjing, 210094, China

[2]Collaborative Innovation Center of Biomedical Functional Materials, Nanjing Normal University, Nanjing, 210046, China

[*]Corresponding Authors: Yinghong Xiao. Email: yhxiao@njnu.edu.cn; Jianfei Che. Email: xiaoche@njust.edu.cn

Received: 08 July 2023 Accepted: 02 November 2023 Published: 11 March 2024

ABSTRACT

The abuse of plastic food packaging has brought about severe white pollution issues around the world. Developing green and sustainable biomass packaging is an effective way to solve this problem. Hence, a chitosan/sodium alginate-based multilayer film is fabricated via a layer-by-layer (LBL) self-assembly method. With the help of superior interaction between the layers, the multilayer film possesses excellent mechanical properties (with a tensile strength of 50 MPa). Besides, the film displays outstanding water retention property (blocking moisture of 97.56%) and ultraviolet blocking property. Anthocyanin is introduced into the film to detect the food quality since it is one natural plant polyphenol that is sensitive to the pH changes ranging from 1 to 13 in food when spoilage occurs. It is noted that the film is also bacteriostatic which is desired for food packaging. This study describes a simple technique for the development of advanced multifunctional and fully biodegradable food packaging film and it is a sustainable alternative to plastic packaging.

KEYWORDS

Chitosan; alginate; layer-by-layer self-assembly; pH-sensitive; multilayer films

1 Introduction

Since the middle of the 20th century, petroleum-based polymers like polyethylene have been extensively employed in the food packaging sector due to their superior mechanical qualities, plasticity, and lightweight [1]. However, petroleum-based polymers show poor biodegradability and reprocessability, which have caused a series of significant environmental contamination and ecological issues [2]. With the improvement of consumers' requirements for food quality, utilizing biopolymers to prepare cost-effective active intelligent films has become a hot research area [3]. The classification of biopolymers is based on their origin and production methods, which can be broadly categorized into three groups: direct extraction from biomass, synthesis of bio-derived monomers and production by microorganisms [4]. In numerous previous studies, polysaccharides (like starch and cellulose) have been extensively investigated as potential substitutes for food packaging materials [5,6].

Among multiple natural polysaccharides, chitosan (CS) is derived from chitin by deacetylation, which can obtained from crustacean shells (such as shrimp and crab), as well as the unique cationic polysaccharide

that exists in nature [7]. The properties of CS such as biodegradability, biocompatibility, non-toxicity, film-forming properties, inherent antibacterial and antioxidant properties allow its application in the food, pharmaceutical and cosmetics industries, especially in food packaging [8]. Many studies have already reported CS-based films with excellent oxygen barrier and permeability-reducing properties [9,10], demonstrating that it has the potential to extend the shelf-life and freshness of products. However, the strong hydrophilicity of CS leads to poor water resistance and thermal properties, limiting its further usage in food packing. Properties such as great strength, insolubility, elasticity, barrier properties, and thermostability are necessary for packaging materials to adapt to various processing conditions [11].

Sodium alginate (SA), which is composed of β-D-mannuronic acid and α-L-guluronic acid linked in a linear (1 → 4) configuration [12], is a natural anionic polysaccharide that can produce electrostatic interaction with cationic polymers (e.g., CS) to improve the mechanical properties and water resistance of CS-based multilayer films [13]. SA improves the water resistance of CS because the WVP (Water Vapor Permeability) of multilaminated films is mainly determined by the WVP of each layer. Since SA is less hydrophilic than CS, the WVP of CS/SA film decreases and the water resistance is better [14,15]. Vieira et al. [16] have reported that CS and SA composite films exhibit significant potential as polysaccharide-based barriers, demonstrating enhanced water resistance and barrier properties.

The development of active packaging films has broad prospects as it not only improves the structure and mechanical properties but can also optimize the efficacy of the composition, providing additional functions for films. Plant polyphenols and extracts are often added as active substances into film matrixes to better maintain the nutrition, freshness and safety of products [17,18]. The excellent antioxidant and antimicrobial properties of anthocyanins can effectively preserve food quality and prolong shelf life. Additionally, the pH-dependent color changes exhibited by anthocyanins enable the films to serve as indicators for monitoring packaged food quality [19]. Hydrophobic interaction and hydrogen bonding between the tannins in anthocyanins and the chitins in CS contribute to the interfacial assembly of anthocyanins on the surface of CS-based films. Simultaneously, the unpaired electrons from hydroxyphenyl in anthocyanins act as hydrogen donors to effectively eliminate various reactive oxygen species and free radicals, endowing them with antioxidant and antibacterial properties [20,21]. Moreover, the colors of anthocyanins can change with pH due to their structural transformations, allowing it to monitor the freshness of foods. Anthocyanins have long been used in active packaging for their pH-sensitive properties [22]. At the same time, anthocyanin's absorption of UV (Ultraviolet) light and its color can greatly increase the film's opacity, which can have a better performance in the food packaging industry.

So far, current studies concerning active intelligent films have mostly focused on coatings or directly cast into films. The coating can form a film directly on the food surface for maximum protection. However, there are potential interactions between the product components and active substances located on the films, more susceptible to leading to film failure and inducing potential health risks. Direct casting is a widely used film manufacturing method due to its easy operation. The casting preparation process is usually divided into several steps: (1) dissolution of CS in an acid solution at a specified pH; (2) mixing with SA solution; (3) stirring to obtain a homogeneous, viscous solution; (4) filtration, sonication, or centrifugation of the solution to remove residual insoluble particles and air bubbles; (5) pouring onto some sort of a flat substrate; (6) drying at a specified temperature, relative humidity, and time; (7) peeling the film off the flat substrate. This method still has certain limitations. Firstly, the blending process of film-forming liquid, particularly when incorporating special materials, may result in a reduction in the Young's modulus of the film [23]. Secondly, prolonged drying time, film shrinkage, brittleness, and uneven distribution of active substances after drying can lead to the formation of "drug islands" and the accumulation of non-drying substances within the film [24]. Using layer-by-layer (LBL) self-assembly technique to fabricate multilayer films offers a new strategy to overcome the limitations of food

packaging films. Likewise, it has been confirmed that multilayer films possess better properties than single-layer ones [25].

In this study, CS/SA composite films were prepared by LBL method, which is more advantageous compared with the traditional casting method, owing to the sustained release of anthocyanins and enhancement of the comprehensive properties of the modified films, such as tensile strength, water resistance and light barrier. The addition of anthocyanins resulted in a significant improvement in the antimicrobial and UV-blocking properties of the films and enabled the films to have pH-indicating capability. This study compared the effects of different anthocyanin contents and different preparation methods on the internal structure, physical properties, antimicrobial and antioxidant properties and pH sensitivity of the films. The fabrication procedure of CS/SA composite films is presented in Scheme 1.

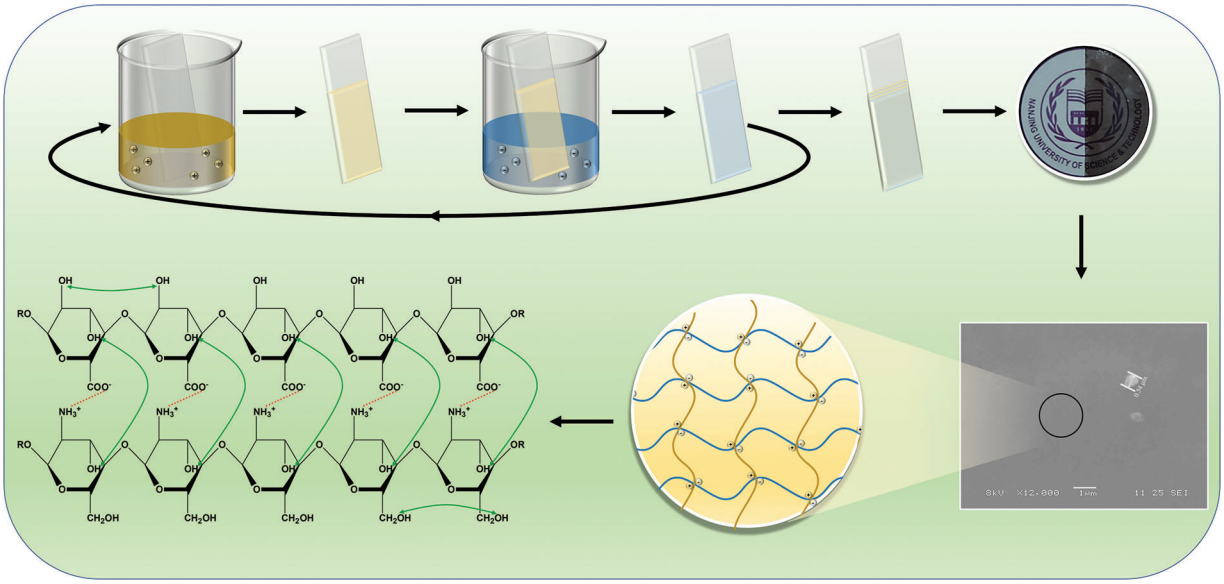

Scheme 1: The fabrication procedure of CS/SA composite films

2 Materials and Methods

2.1 Materials

Acetic acid and pH buffers (pH 4.79) were purchased from Sinopharm Chemical Reagent Co., Ltd. (Shanghai, China). CS, with a deacetylated degree of 90%, glycerol, 2,2′-azino-bis(3-ethyl-benzothiazoline-6-sulfonic acid) (ABTS) and other pH buffers were purchased from Shanghai Aladdin Bio-chem Technology Co., Ltd. (Shanghai, China). SA was provided by J&K Scientific Co., Ltd. (Beijing, China). Anthocyanins (Source Blueberry anthocyanin, 5%–25%) and potassium persulfate were purchased from Shanghai Macklin Biochemical Co., Ltd. (Shanghai, China).

2.2 Preparation of Film-Forming Solution

First, 3 g CS powder was dissolved in the 3 wt% acetic acid solution and stirred at room temperature for 6 h to prepare a 3 wt% CS acetic acid aqueous solution. Subsequently, different amounts of anthocyanins (0%, 20%, 30% and 40% w/w based on CS) were individually added into CS acetic acid aqueous solution, followed by adding glycerol into the film-forming solution (30% w/w based on CS) as a plasticizer, and the mixture was stirred for 2 h. The same method was used to prepare a 3 wt% SA solution without anthocyanins in deionized (DI) water.

2.3 Preparation of CS/SA Films

CS/SA films were developed following the method of Şenel et al. with some modifications [26,27]. CS/SA multilayer films were assembled according to the following procedure: the slides were pre-treated with 5% sodium hydroxide solution and then immersed in the CS solution for 10 min, followed by washing with DI water and then dried. Thereafter, the slides were immersed in SA solution for 10 min, followed by washing with DI water and then dried, thus a bilayer was prepared. The above process was repeated 6 times to obtain multilayer films, which were named 0%L, 20%L, 30%L and 40%L depending on the anthocyanin content, respectively. The films were carefully detached from the sheet and air-dried for 48 h at room temperature. Subsequently, it was transferred to a dryer containing a saturated solution of Ca $(NO_3)_2$ and maintained at 50% relative humidity for another 48 h. The CS films with different contents of anthocyanins were prepared by casting method as the control groups, named 0%C, 20%C, 30%C and 40%C, respectively.

2.4 Fourier Transform Infrared Spectrometry (FTIR)

FT-IR spectroscopy (NICOLETIS10, Thermo Fisher Scientific Co., LTD., USA) was determined by Attenuated Total Refraction to observe the structural interactions of CS composite films. The spectra were collected in a wavenumber range of 4000–400 cm^{-1} by averaging 32 scans at a resolution of 4 cm^{-1}.

2.5 Thickness, Moisture Content, Swelling Degree and Water Solubility

The thickness was measured by a digital thickness gauge (32CHQF2530, Syntex, Zhejiang, China) with a minimum division value of 0.1 μm.

The moisture content (MC (%)), swelling degree (SD (%)) and water solubility (WS (%)) were characterized by the following steps [28]: The samples were weighed (M_1) and dried at 105°C for 24 h until a constant weight (M_2) was achieved. Subsequently, the samples were immersed in 30 mL of DI water for 24 h and weighed again (M_3). The undissolved samples were dried at 105°C for another 24 h and M_4 was measured. The MC, SD and WS were calculated according to the following equations:

$$MC(\%) = \frac{M_1 - M_2}{M_1} \times 100 \tag{1}$$

$$SD(\%) = \frac{M_3 - M_2}{M_2} \times 100 \tag{2}$$

$$WS(\%) = \frac{M_2 - M_4}{M_2} \times 100 \tag{3}$$

2.6 Morphological Characteristics

The surface morphologies of the composite films were observed using an ultra-high resolution thermal emission scanning electron microscope (SEM, Thermo Scientific Apreo 2S) at an acceleration voltage of 15 kV. Each sample was attached to cylindrical aluminum stubs with a double-sided tape and sputtered with a thin gold layer.

2.7 Mechanical Properties

The tensile strength (TS) and elongation at break (EAB) were evaluated using a texture analyzer machine (CMT-4254, Jinan HengXu Testing Machine Technology Co., Ltd., Jinan, China). The gauge lengths were 10 mm and the crosshead speed used was 1 mm/min.

2.8 Optical Properties

A UV-Vis spectrophotometer (UV-1800, Shimadzu, Kyoto, Japan) was used to measure light transmission at wavelengths between 200–800 nm. The opacity was determined by measuring absorbance at 600 nm and calculated using the given equation.

$$\text{Opacity} = \frac{A_{600}}{d} \tag{4}$$

where A_{600} is the value of absorbance at 600 nm, and d is the film's thickness (mm).

2.9 Antimicrobial Properties

The antimicrobial properties of CS/SA composite films were examined by using the agar diffusion method [29]. The strain was provided by the Laboratory of the School of Environment and Biology, Nanjing University of Science and Technology. *Escherichia coli* (E. coil), a representative Gram-negative bacterium, was selected for antimicrobial testing. First, 10 mL of E. coil bacterial solution containing 10^5–10^6 CFU/mL was inoculated on agar medium and then a 10 mm diameter film was placed on the medium and incubated at 37°C for 24 h. Finally, the inhibition zone was recorded to evaluate the antibacterial effect.

2.10 Antioxidant Activity

The antioxidant activity of CS-based composite films was determined by the $ABTS^{+}$• assay according to the previously described method. ABTS solution was prepared by adding 10 mg of ABTS to 2.6 mL of potassium sulfate (2.45 mmol/L) solution to a concentration of 7 mmol/L. The obtained solution was incubated at room temperature for 16 h to allow the generation of free radicals ($ABTS^{+}$•) in dark conditions. And the solution was further diluted with milli-Q water and maintained at an absorbance of 0.70 ± 0.20 at wavelength 734 nm. A membrane sample with a concentration of 1.0 mg/mL was followed by mixing with 3 mL of $ABTS^{+}$• solution and incubating for 1 h at room temperature. Ultimately, the absorbance was recorded at 734 nm using a UV-Vis spectrophotometer. Using deionized water as a baseline, the scavenging activity of ABTS radicals was determined according to the following equation:

$$\text{Antioxidant activity } (\%) = \frac{A_0 - A_1}{A_0} \times 100 \tag{5}$$

where A_0 is the absorbance of $ABTS^{+}$• solution mixed with DI water, A_1 is the absorbance of the membrane sample mixed with $ABTS^{+}$• solution.

2.11 pH Sensitivity

To determine the pH-sensitivity of anthocyanins solution, 2 mg of anthocyanins was dissolved in 20 mL of different buffers (pH = 1–13). The obtained extract anthocyanins solutions were scanned in the 400–800 nm using a UV-Vis spectrophotometer. The pH sensitivity of films was evaluated by immersing film samples in different buffers (pH = 1–13).

3 Results and Discussion

3.1 FTIR

The FTIR spectra of CS/SA composite LBL films are shown in Fig. 1. The broad bands at 3600–3000 cm^{-1} in the spectra represent overlapping stretching vibrations of O-H and N-H of CS and SA [30]. The peaks at 1645, 1540 and 1338 cm^{-1} correspond to the C=O stretching vibration, amide II groups of CS (N-H inplane bending vibration) and amide III of CS (C-N stretching vibration), respectively. The

1400 and 1020 cm^{-1} peaks of SA are attributed to COO^- and stretching vibration of C-O-C [31]. The infrared signals of $-NH_3^+$ in CS and $-COO^-$ in SA indicate varying degrees of ionization for the amino group in CS and the carboxyl group in SA, which contributes to the formation of a polyelectrolyte network between them.

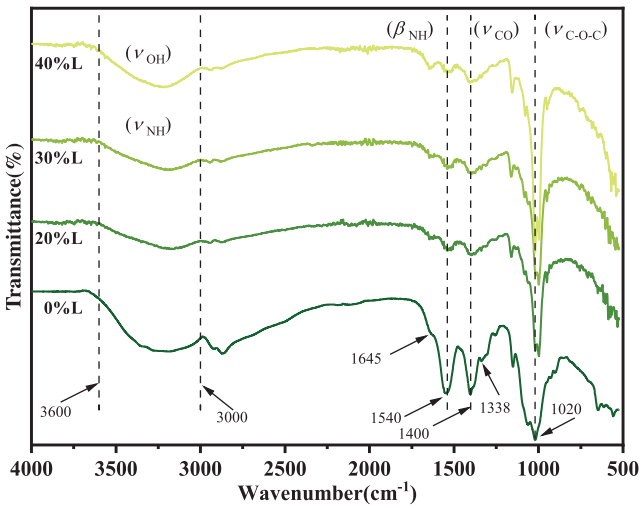

Figure 1: FTIR spectra of CS/SA composite LBL films with different anthocyanin content

The fundamental building block of anthocyanins consists of polyaromatic phenols, and its characteristic skeletal vibration is primarily localized in the range of 1520–1540 cm^{-1} and 700–850 cm^{-1}. These distinctive peaks align with those observed in CS/SA composite films, posing challenges for their differentiation [32]. However, the peak at 3600–3000 cm^{-1} was slightly shifted to a low wavenumber after adding anthocyanidin as a result of formation of hydrogen bonds among anthocyanins and CS and SA chains. Simultaneously, the bands at 1540 and 1400 cm^{-1} became broader, probably due to the existence of electrostatic interactions between the CS and SA layers.

3.2 Thickness, MC, SD and WS

Several physical properties of films, such as transparency and tensile strength, are directly affected by thickness, making thickness an important variable in evaluating food packaging films. As shown in Fig. 2a, the thickness of casting films (37.7 ± 5.66 to 83.8 ± 3.79 μm) is thinner than that of LBL films (76.8 ± 6.34 to 101.6 ± 3.92 μm). The thickness of film samples mainly depends on the compositions of the film-forming solutions and the force between the film-forming materials [33]. The difference in film thickness with the same composition of the film-forming solution suggested that LBL can lead to enhanced interaction forces between polyelectrolytes, which is consistent with the results that the TS of LBL films is higher than that of casting films in mechanical properties studies. On one hand, anthocyanins can form hydrogen bonds with CS and SA, while their steric hindrance surpasses that of CS and SA, leading to an increased thickness of the film. On the other hand, the additive contains 5%–25% anthocyanin content, which is lower than that of the substrate. Overall, the effect of adding anthocyanins on the film thickness was less than that of the preparation methods.

MC reflected the ability of the films to absorb moisture from a relatively high-humidity environment to maintain a moderate internal balance, thereby assessing the film's ability to resist internal water loss. The addition of anthocyanins resulted in a decreasing trend of film MC, mainly due to the formation of hydrogen bonds between CS/SA chains and anthocyanins and displacing a portion of the CS and SA interacting with moisture.

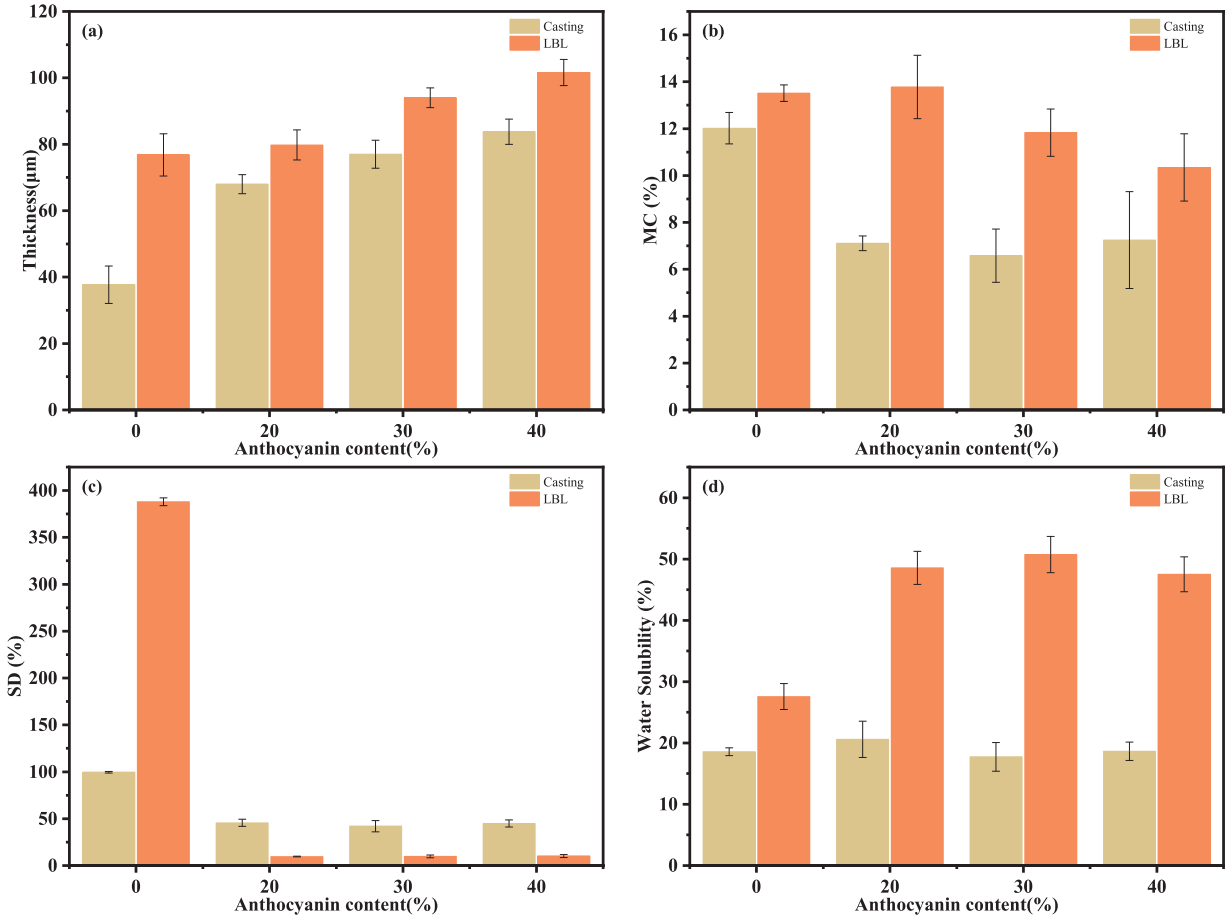

Figure 2: (a) Thickness, (b) MC, (c) SD and (d) WS of film samples

The swelling behavior of the films involved the formation and dissociation of hydrogen bonds, the ionization of carboxyl/amino groups and the diffusion of water, reflecting the hydrophilicity of the films. In general, low SD allowed the films to maintain a stable tensile strength by ensuring the structure stability in a wet environment, as deformation and the insertion of water molecules are very detrimental to practical use. In both casting and LBL films, the addition of anthocyanins significantly reduced the SD, especially in LBL films by up to 97.56%. The interactions between the CS/SA layers and the water molecules during swelling increase molecular spacing and volume, while anthocyanins form hydrogen bonds with CS/SA and partly prevent the interactions with moisture.

WS is an important indicator for evaluating the water resistance of the films. As summarized in Fig. 2d, it can be noted that the WS of the films appeared to increase and then decrease with the addition of anthocyanins. The hydrophilic properties of anthocyanins and substances such as water-soluble vitamins contained in the blueberry extract are the main drivers of the increase in WS. A phenomenon similar to the increase in WS is also present in the pH-responsive smart films based on CS-methylcellulose matrix integrated with phyllanthus reticulatus ripen fruit anthocyanin [34]. The reduction in WS, on the other hand, is associated with a decrease in the accessible hydroxyl groups in films, as a consequence of the interaction with the oxygen functional groups in the blueberry extract, leading to a decrease in the affinity of the film to adsorb water. A similar decrease in WS has been reported for other films containing plant extracts [35,36]. When different mass fractions of anthocyanins and composite films are considered, the

dominant roles of the two effects are different. The competing effects of the two interactions caused the WS to first increase and then decrease.

3.3 Morphological Characteristics

As shown in Fig. 3a, the composite films were homogeneous in all phases and appeared reflective under light conditions, indicating that the film surfaces were quite flat and smooth. The left side of the film image displays samples without the addition of anthocyanins, whereas the right side exhibits films with varying levels of incorporated anthocyanin content. The films' color on the right gradually deepened as the anthocyanin content increased. Furthermore, LBL films exhibited darker colors than casting films under the same formulation, providing a better UV/Vis light barrier, which corresponded to the results of opacity analysis. There was no unevenness, microporosity or cracking under the naked eye, regardless of the amount of anthocyanin. And the letters and patterns on the underside of the films were still clearly recognizable, which was very helpful in showing the characteristics of the item itself.

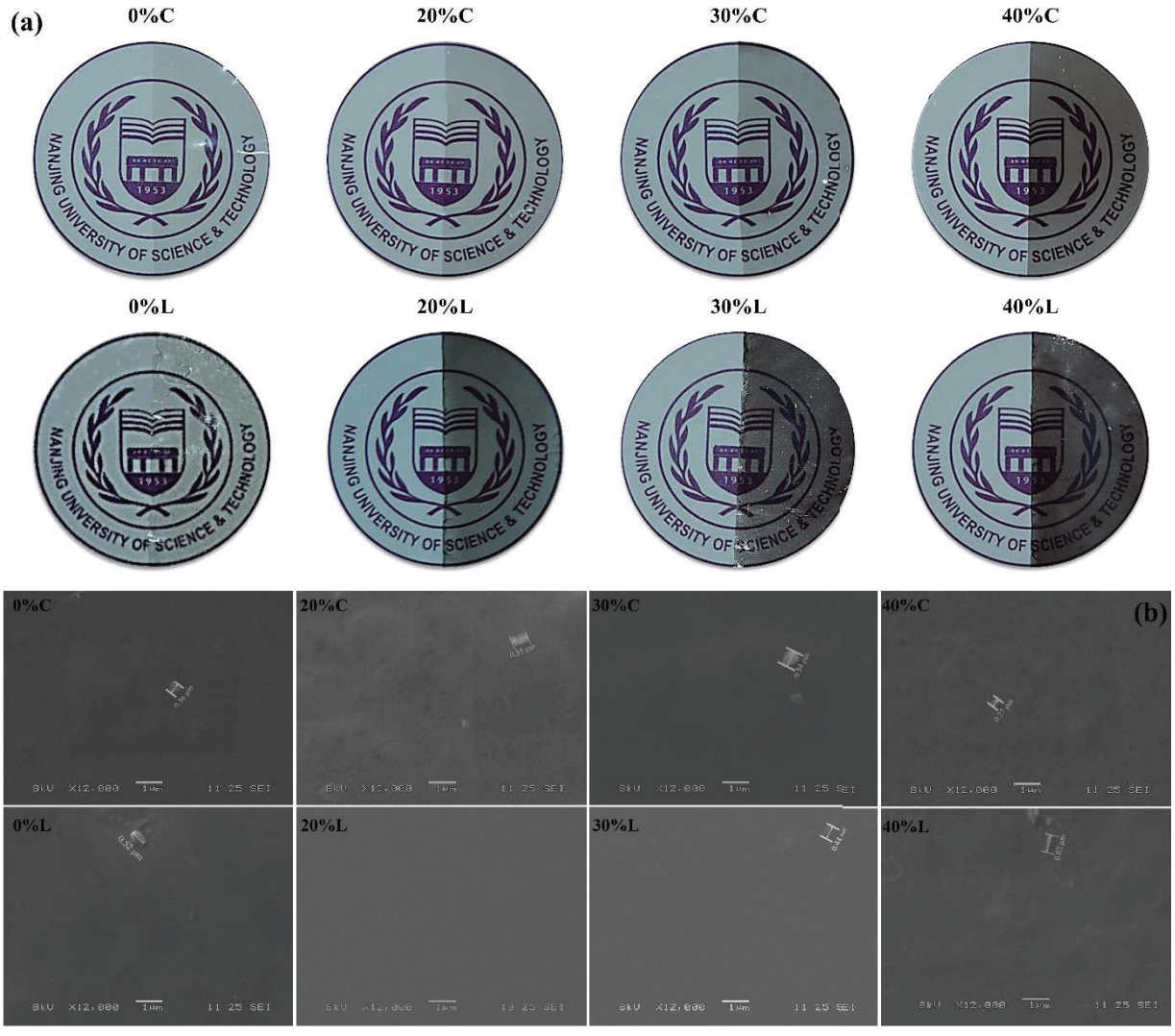

Figure 3: (a) Image and (b) SEM of film samples

The surface morphology of the films was examined using SEM to investigate the incorporation of anthocyanins into composite films. The different components and their drying behavior significantly influence the process of molecular assembly, consequently impacting the microstructure of the film [37]. Analysis of the different samples indicated smooth and continuous surface of the films [38], on account of the strong hydrogen bonding interaction between CS, SA and anthocyanins. Extremely small amounts of particles below 0.6 μm in size appeared on the film surface, owing to partially unmelted particles such as CS, blueberry extract, etc. [39]. Additionally, the presence of corrugations on the film surface might be attributed to the hydrogen bonds between the substrates, a phenomenon commonly observed in studies pertaining to CS composite films [40]. The film samples exhibited a compact and homogeneous structure, devoid of any pores or cracks. This is a full demonstration of the fact that the anthocyanins as well as the plasticizer glycerol were dispersed quite uniformly into the film matrix. Numerous holes, structural discontinuities, surface roughness and other phenomena would appear when CS was applied to prepare composite films with other plant extracts such as garlic extract, rosehip seed extract, and summer cress extract [41,42]. These defects had a negative impact on the mechanical properties, water and oxygen barrier of the film. Apparently, the films prepared by our research could well circumvent such problems and contribute to the further advancement of practical use.

3.4 Mechanical Properties

During processing, transportation, and storage, the mechanical properties of packaging materials play a crucial role in their ability to endure stress and uphold the structural integrity of the product. In terms of general, TS and EAB are important parameters for assessing the mechanical properties of composite films. The TS and EAB of composite films with different preparation methods and anthocyanin contents are shown in Fig. 4.

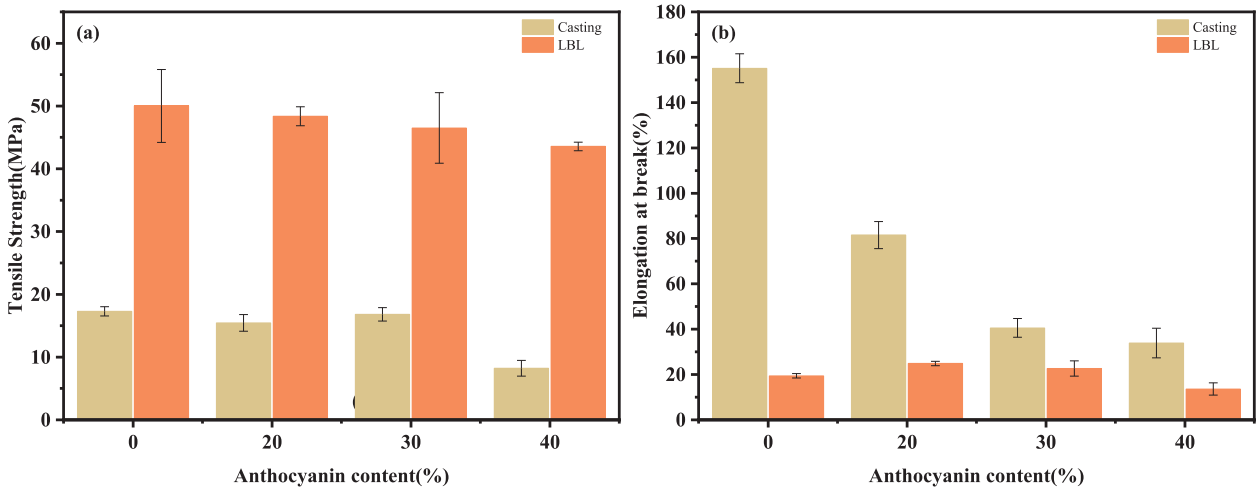

Figure 4: (a) TS and (b) EAB of film samples

TS of LBL films showed significant enhancement compared to casting films, particularly when the anthocyanin addition reached 40%. In this case, TS of LBL films exhibited >5 folds of casting films. (40%C: 8.22 ± 1.25 MPa; 40%L: 43.6 ± 0.68 MPa). The significant increase in TS is attributed to the strong intermolecular interaction between the membrane matrix molecules by LBL, leading to a tighter structure [43]. The results are consistent with the opacity analysis. The enhancement effect of the LBL

method, however, is what restricted the movement of matrixes and elevated film rigidity, leading to an increase in TS and a decrease in EAB of LBL films.

Unfortunately, the TS and EAB of the films tended to decrease after the addition of anthocyanins.

In general, the incorporation of hydroxyl-containing substances enhances intermolecular interactions. However, in the case of anthocyanins and the film matrix, intramolecular bonds are predominantly formed instead of intermolecular bonds. This leads to phase separation among different components and hampers the interactions between polymer chains during drying, thereby disrupting the ordered structure of the film and consequently diminishing its mechanical properties [44,45]. Kaya et al. showed the same phenomenon decreasing TS of CS composite films as the extracted content increased [46].

But it is evident that the TS values of the casting films are more influenced by the anthocyanin content, while the LBL films are relatively stable. The possible reason is that during the process of LBL self-assembly, a greater number of intermolecular interactions occur between anthocyanins and polymer matrix molecules, thereby impeding the occurrence of system inhomogeneity.

3.5 Optical Properties

The consideration of light transmittance and opacity holds paramount importance in the advancement of food packaging materials. The film could be suitable for packaging materials of light-sensitive foods by appropriately reducing light transmission and increasing opacity, thus providing effective light protection properties [47]. Therefore, the light transmittance and opacity of the films were studied, and the results are shown in Fig. 5.

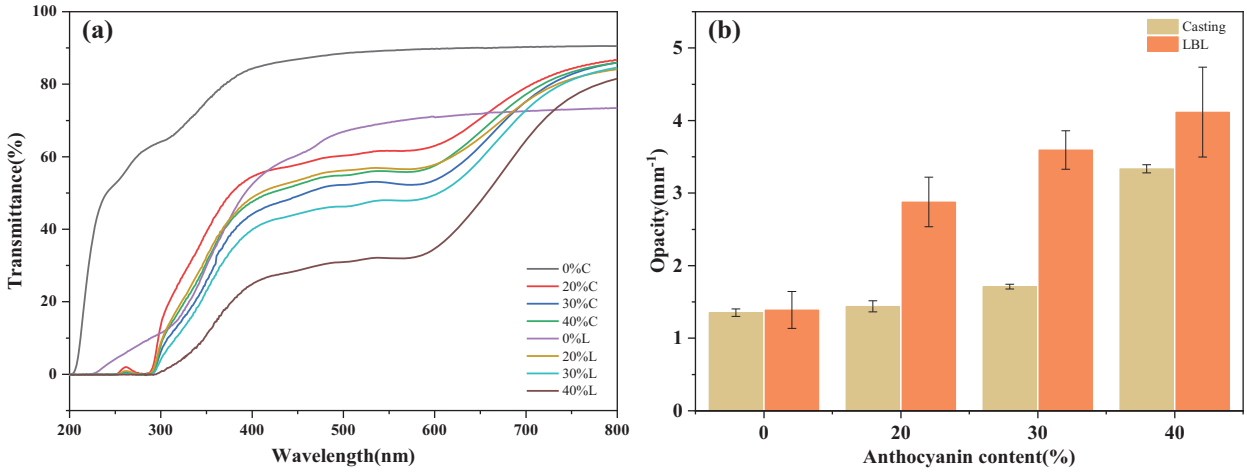

Figure 5: (a) Light transmittance and (b) opacity of film samples

The incorporation of anthocyanins into the films significantly decreased the transmittance in the UV and visible light range compared to the control films, due to the fact that anthocyanins are inherently colored and have a good ability to absorb UV rays [48,49]. UV region light waves (200–380 nm) were prone to oxidation of lipids, and the films had the largest drop in light transmittance in the range of 200 to 300 nm, which had significant meaning for effectively inhibiting photounstable food components such as lipids from oxidation [50]. The reduction can be attributed to the high number of unsaturated bonds present in anthocyanins, which exhibit a strong absorption effect on UV/Vis light [51]. In addition, the light transmission of LBL films is lower than that of casting films with the same anthocyanins concentration, and the value of the difference became more significant with the increase of anthocyanin concentration. The results provided sufficient

evidence that the LBL method is more conducive to the improvement of the UV-Vis light barrier performance of the films.

In agreement with the appearance (Fig. 5a), both the LBL preparation method and the addition of anthocyanins significantly improved the film opacity. The most significant improvement in opacity is a 196.18% enhancement in the 40%L films (from 1.39 to 4.12 mm^{-1}). One reason for this is the increment of the thickness of the films, another reason is that blueberry anthocyanin itself showed a blue-purple color. Wang et al. [52] reported that pine bark extract rich in proanthocyanidins is able to reduce the opacity of CS films in a related study.

3.6 Antimicrobial Properties

The antibacterial activity of films was assessed by determining the presence or absence of an observable inhibition zone surrounding the film following incubation [53]. The inhibition zone diameters yielded by composite films with different anthocyanin concentrations and preparation methods against E. coli are shown in Fig. 6. The antimicrobial activity of LBL films was assessed by employing casting films, with PE films and casting films serving as the control group.

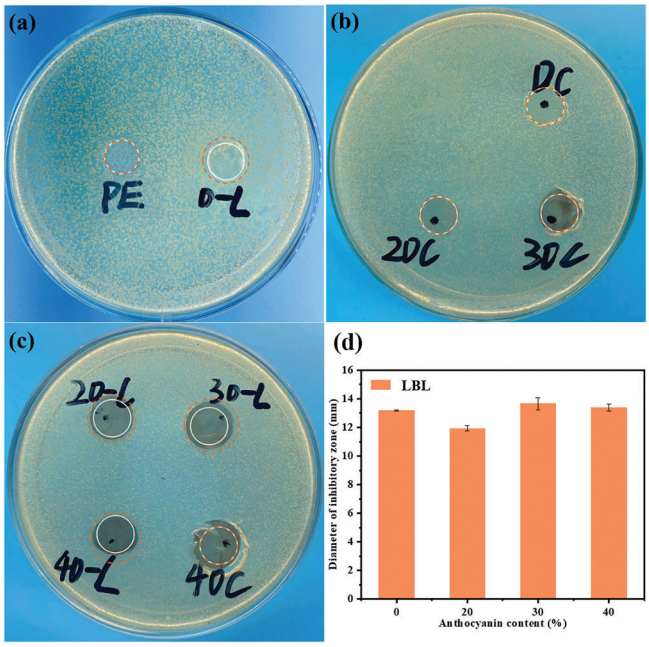

Figure 6: Antimicrobial properties of film samples

The results disclosed that all LBL films effectively inhibited the bacterial growth for the presence ofinhibition zones around the films. In contrast, PE and casting films showed no inhibition zones and even obvious folds and ruptures were produced. Inhibition zone diameters for all films were calculated and shown in Fig. 6d. The prevailing view believed that the antibacterial activity of CS is due to the $-NH_3^+$ groups providing positive to films [54]. The $-NH_3^+$ interacted electrostatically with the main component of bacteria, namely the anionic phospholipid dipalmitoyl phosphatidylglycerol. This interaction resulted in increased permeability of bacteria cell membranes, promoting the release of nucleic acid, glucose and lactate dehydrogenase from the cells, disrupting the transport of nutrients to the cells, and finally the death of bacterial [55]. Moreover, only the dissolved CS molecules can diffuse in agar gel and cause the formation of an inhibition zone. CS molecules immobilized in film matrixes could not

produce an inhibition zone because they could not diffuse [56]. On the one hand, the complexation of CS with SA, where the negatively charged groups in films interacted with the amide groups, resulting in the disruption of the peptide bonds in the tetrapeptide bridge and the disruption of the cell membrane [57]. Consequently, the films would be suitable for packaging fresh food containing water such as vegetables and meat [58].

The antimicrobial performance of the films showed no significant enhancement after the addition of anthocyanins. It is plausible that the interaction between polymer matrix molecules and anthocyanins impedes the release of anthocyanins.

3.7 ABTS $^{+}$• Scavenging Activity

ABTS is a somewhat standard reagent that has been widely used to detect the ability of compounds to act as free radical scavengers. As shown in Fig. 7a, ABTS could be triggered by $K_2S_2O_8$ and one-electron oxidation yields glaucous $ABTS^{+}$• free radical, with a absorbance peak at 734 nm. Incubation of this glaucous $ABTS^{+}$• radical solution with composite films led to a gradual lightening or even disappearance of the glaucous color, which meant that the $ABTS^{+}$• radical was quenched by the antioxidant components of the films [59]. The attenuation of the color could be easily determined by spectrophotometry.

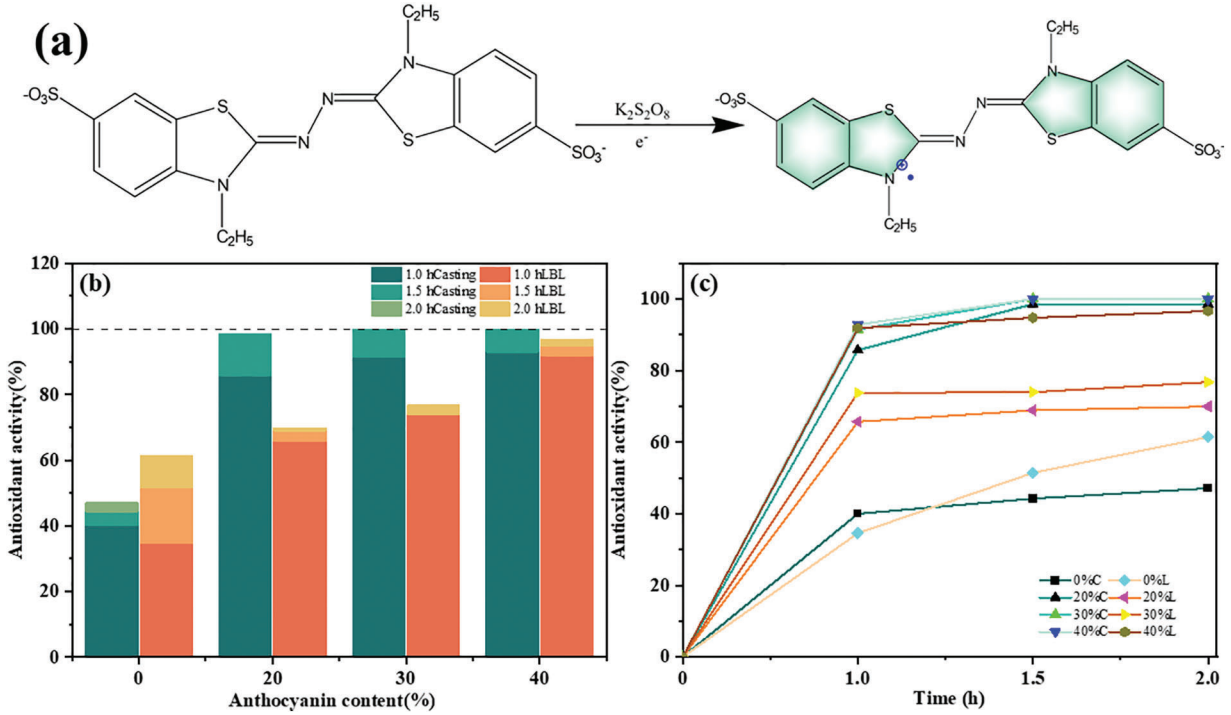

Figure 7: (a) $ABTS^{+}$• free radical generation, (b) antioxidant activity of film samples and (c) changes in antioxidant activity with time

Figs. 7b and 7c present $ABTS^{+}$• free radical scavenging activity of different films and their changes with time. The free radical scavenging rates of 0%C and 0%L films after 2 h incubation are 47.14% and 61.42%, respectively, which indicated that CS composite films possessed certain antioxidant activity. The antioxidant mechanism of CS is first attributed to the formation of stable macromolecular radicals between its residual free amino groups and $ABTS^{+}$• radicals. Secondly, the -OH groups as well as the -COOH groups in SA and CS could scavenge free radicals [60]. The antioxidant activity of films showed a significant rise after adding

anthocyanins. Most films could reach more than 70% oxidation rate after 2 h incubation and even reach 100% at 30%C and 40%C. The reason for this is the high content of polyphenolic compounds in anthocyanins, which are considered to be the most powerful oxidants and effective in scavenging free radicals [61].

As shown in Fig. 7b, the casting films exhibited stronger antioxidant capacity than the LBL films after 1 h incubation. The amino groups of CS were not occupied in casting films while the amino groups of CS in LBL films connected with the carboxyl groups in SA to form a tight network structure, making its antioxidant ability inferior to that of the casting films. In addition, SD of the films is a key factor affecting the release of active agents [62]. High SD facilitates the rapid release of antioxidants, consistent with the results of the SD analysis mentioned above.

We observed an explosive increase in the antioxidant activity of all films during the initial stage (Fig. 7b). And its rate increased with the increase in anthocyanin content. When the antioxidants in the films are released, free radicals can be rapidly inhibited or quenched, resulting in a rapid increase in antioxidant activity. The antioxidant activity of each film enhanced relatively slowly after incubation for 1 h and seemed to reach a plateau period. And the amount of anthocyanin addition in casting films had no additional accelerated effect on the gain of antioxidant activity due to this activity is limited by the kinetics of release after 1 h, which is further verified by Benbettaïeb et al. [60] through the effect of release kinetics on antioxidant activity.

Efficient free radical scavenging capabilities are expected for packaging films. It is also important to guarantee a stable and sustained release of antioxidants from an antioxidant-active packaging film during food storage [63]. For example, the carboxyl group of gallic acid partially reacts with CS during the compounding process and cannot be released, resulting in reduction in its sustained release. The rapid release of antioxidant substances in the early stage is not conducive to long-term recycling. Although 0%L, 20%L and 30%L showed sustained release behavior, the antioxidant capacity remained below 80% throughout the late stage. For this reason, 40%L is more advantageous in terms of combining both oxidation resistance and sustained release properties.

According to the above analyses, LBL films exhibited more excellent mechanical properties, light barrier, thermal stability, antimicrobial activity, sustained release properties, and significantly reduced swelling, making them more suitable for humid environments. In this regard, LBL films were used for the follow-up study.

3.8 pH-Sensitivity

As shown in Fig. 8a, anthocyanins underwent structural transformation with pH changing. This property endows anthocyanins with pH sensitivity, making them active substances that can detect changes of pH. Furthermore, the transformation of the anthocyanins' structure can lead to color changes being quantitatively detected by a UV-Vis spectrophotometer.

The color changes of anthocyanins and the composite filems at different pH values (pH = 1–13) are shown in Fig. 8b. The anthocyanin solution appeared red at pH = 1 and gradually transformed to pink and purple with the increase of pH. The color suddenly turned brown at pH = 10 and finally became yellow at pH = 12–13. This is the result of the degradation of anthocyanins under strong alkaline conditions [64]. The color changes of the anthocyanin solution corresponded to the structural alteration, from red flavonoid cations to colorless methanolic pseudobases, blue quinolones, and yellow chalcones. A mixture of red flavylium cation and yellow chalcone ions can coexist at a pH value between the values when the equilibrium forms predominate, which allows for a combination of their colors and shows other colors [65]. At the bottom of Fig. 8b, composite films exhibited obvious color changes in different buffer solutions. The time required for the color changes of composite films when immersed in buffer solutions

is approximately 3–5 s. Especially at pH = 1 and pH = 13, the differences of the colors of the films are more pronounced when the soaking time is longer.

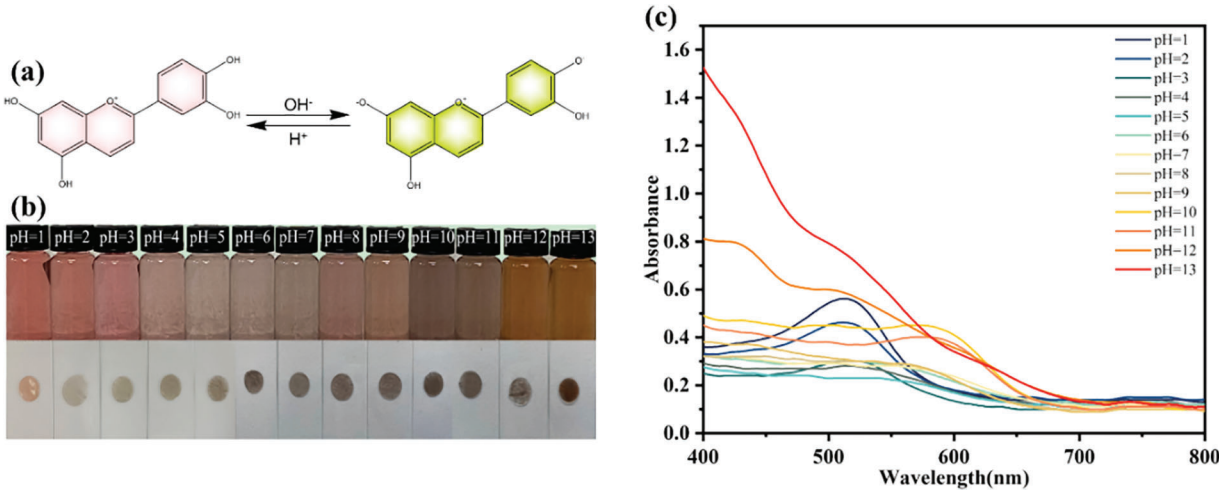

Figure 8: (a) structural transformation of anthocyanins under acidic and alkaline conditions, (b) color changes of anthocyanin solution and composite film at pH = 1–13 and (c) UV-Vis spectra of anthocyanins at pH = 1–13

The corresponding UV–Vis spectra of anthocyanins in different buffer solutions are presented in Fig. 8c. At pH = 1–4, the maximum value of the absorption appeared at 530 nm, and the absorption intensity of the solution gradually decreased as the pH became more basic. When the pH increased from 4 to 11, the absorption peaks gradually shifted to 580 nm and the absorption intensity enhanced continuously. One of the most important features of the changes in the freshness of food is the pH transformation. Fast and sensitive smart packaging films can provide timely detection and feedback on the freshness of items.

4 Conclusion

In summary, we designed a pH-sensitive multifunctional film by introducing anthocyanin as pH indicative factor into CS and SA via the LBL method. Benefiting from the electrostatic interaction and hydrogen bonding between chitosan and sodium alginate, the film exhibits a rosy tensile strength of 50 MPa and UV blocking property which outperforms the traditional casting sample. The addition of anthocyanin endows the film with a visual indication to judge the food spoilage within a wide range of pH changes. At the same time, anthocyanin enhances the water resistance by reducing the free hydroxyl group in films and increases the water resistance to 97.56%. Moreover, the film enjoys favorable bacteriostatic, which is attributed to the positive charge release from CS promoted by anthocyanins and sodium alginate. Our film is very attractive as a base material to replace plastic packaging in common consumer products such as wrap or other applications in contact with food.

Acknowledgement: This work was financially supported by the the National Undergraduate Training Program for Innovation and Entrepreneurship of China.

Funding Statement: National Undergraduate Training Program for Innovation and Entrepreneurship of China (Grant No. 202210288027).

Author Contributions: Mingxuan He (Data curation: Lead; Investigation: Lead; Validation: Lead). Jianfei Che, Yinghong Xiao (Conceptualization: Lead; Formal analysis: Lead; Funding acquisition: Lead; Project administration: Lead; Supervision: Lead; Visualization: Lead; Writing–original draft: Lead; Writing–review & editing: Lead). Jiaming Shen, Yahui Zheng, Yongzheng Zhang, Jiawei Shi (Investigation: Supporting; Validation: Supporting; Formal analysis: Supporting; Writing–original draft: Supporting; Writing–review & editing: Supporting).

Availability of Data and Materials: The data that support the findings of this study are available from the corresponding author upon reasonable request. All the materials used in our experiment can be purchase from the manufacturers.

Conflicts of Interest: The authors declare that they have no conflicts of interest to report regarding the present study.

References

1. Naseri, H. R., Beigmohammadi, F., Mohammadi, R., Sadeghi, E. (2020). Production and characterization of edible film based on gelatin-chitosan containing Ferulago angulate essential oil and its application in the prolongation of the shelf life of turkey meat. *Journal of Food Processing and Preservation, 44(8),* 14558. https://doi.org/10.1111/jfpp.14558
2. Hong, M., Chen, E. Y. X. (2019). Future directions for sustainable polymers. *Trends in Chemistry, 1(2),* 148–151. https://doi.org/10.1016/j.trechm.2019.03.004
3. Park, S., Oh, K. K., Lee, S. H. (2019). Biopolymer-based composite materials prepared using ionic liquids. *Advances in Biochemical Engineering/Biotechnology, 168,* 133–176. https://doi.org/10.1007/10_2018_78
4. Lisitsyn, A., Semenova, A., Nasonova, V., Polishchuk, E., Revutskaya, N. et al. (2021). Approaches in animal proteins and natural polysaccharides application for food packaging: Edible film production and quality estimation. *Polymers, 13(10),* 1592. https://doi.org/10.3390/polym13101592
5. Tibolla, H., Feltre, G., Sartori, T., Czaikoski, A., Pelissari, F. M. et al. (2021). Shelf life of cashew nut kernels packed in banana starch-based nanocomposites. *International Journal of Food Science and Technology, 56(8),* 3682–3690. https://doi.org/10.1111/ijfs.14920
6. Bof, M. J., Laurent, F. E., Massolo, F., Locaso, D. E., Versino, F. et al. (2021). Bio-packaging material impact on blueberries quality attributes under transport and marketing conditions. *Polymers, 13(4),* 481. https://doi.org/10.3390/polym13040481
7. Jankar, J., Nagargoje, Y., Chavan, Y., Jankar, J., Sahoo, A. K. (2020). Development of shrimp-based chitosan film and assessment of its mechanical, barrier and antimicrobial properties. *E3S Web of Conferences, 170,* 04003. https://doi.org/10.1051/e3sconf/202017004003
8. Li, S., Wang, H., Wan, Z., Guo, Y., Chen, C. et al. (2022). Strong, water-resistant, and ionic conductive all-chitosan film with a self-locking structure. *ACS Applied Materials and Interfaces, 14(20),* 23797–23807. https://doi.org/10.1021/acsami.2c01118
9. Kumbunleu, J., Rattanapun, A., Sapsrithong, P., Tuampoemsab, S., Sritapunya, T. (2020). The study on chitosan coating on poly(lactic acid) film packaging to extend vegetable and fruit life. *IOP Conference Series. Materials Science and Engineering, 811(1),* 12021. https://doi.org/10.1088/1757-899X/811/1/012021
10. Miranda, S. P., Garnica, O., Lara-Sagahon, V., Cárdenas, G. (2004). Water vapor permeability and mechanical properties of chitosan composite films. *Journal of the Chilean Chemical Society, 49(2),* 173–178. https://doi.org/10.4067/s0717-97072004000200013
11. Wu, X., Luo, Y., Liu, Q., Jiang, S., Mu, G. (2019). Improved structure-stability and packaging characters of crosslinked collagen fiber-based film with casein, keratin and SPI. *Journal of the Science of Food and Agriculture, 99(11),* 4942–4951. https://doi.org/10.1002/jsfa.9726

12. Chen, J., Wu, A., Yang, M., Ge, Y., Pristijono, P. et al. (2021). Characterization of sodium alginate-based films incorporated with thymol for fresh-cut apple packaging. *Food Control, 126,* 108063. https://doi.org/10.1016/j.foodcont.2021.108063
13. Su, W., Yang, Z., Wang, H., Fang, J., Li, C. et al. (2022). Synergistic effect of sodium alginate and lignin on the properties of biodegradable Poly(vinyl alcohol) mulch films. *ACS Sustainable Chemistry and Engineering, 10(36),* 11800–11814. https://doi.org/10.1021/acssuschemeng.2c02290
14. Zhuang, C., Jiang, Y., Zhong, Y., Zhao, Y., Deng, Y. et al. (2018). Development and characterization of nano-bilayer films composed of polyvinyl alcohol, chitosan and alginate. *Food Control, 86,* 191–199. https://doi.org/10.1016/j.foodcont.2017.11.024
15. Cho, S. Y., Park, J. W., Rhee, C. (2002). Properties of laminated films from whey powder and sodium caseinate mixtures and zein layers. *LWT—Food Science and Technology, 35(2),* 135–139. https://doi.org/10.1006/fstl.2001.0826
16. Vieira, T. M., Moldão-Martins, M., Alves, V. D. (2021). Design of chitosan and alginate emulsion-based formulations for the production of monolayer crosslinked edible films and coatings. *Foods, 10(7),* 1654. https://doi.org/10.3390/foods10071654
17. Zhu, F. (2021). Polysaccharide based films and coatings for food packaging: Effect of added polyphenols. *Food Chemistry, 359,* 129871. https://doi.org/10.1016/j.foodchem.2021.129871
18. Rahim, M. A., Ejima, H., Cho, K. L., Kempe, K., Müllner, M. et al. (2014). Coordination-driven multistep assembly of metal-polyphenol films and capsules. *Chemistry of Materials, 26(4),* 1645–1653. https://doi.org/10.1021/cm403903m
19. Yong, H., Liu, J. (2020). Recent advances in the preparation, physical and functional properties, and applications of anthocyanins-based active and intelligent packaging films. *Food Packaging and Shelf Life, 26,* 100550. https://doi.org/10.1016/j.fpsl.2020.10550
20. Wang, P., Liu, J., Zhuang, Y., Fei, P. (2022). Acylating blueberry anthocyanins with fatty acids: Improvement of their lipid solubility and antioxidant activities. *Food Chemistry: X, 15,* 100420. https://doi.org/10.1016/j.fochx.2022.100420
21. Luo, Y., Liu, H., Yang, S., Zeng, J., Wu, Z. (2019). Sodium alginate-based green packaging films functionalized by guava leaf extracts and their bioactivities. *Materials, 12(18),* 108063. https://doi.org/10.3390/ma12182923
22. Sun, J., Jiang, H., Wu, H., Tong, C., Pang, J. et al. (2020). Multifunctional bionanocomposite films based on konjac glucomannan/chitosan with nano-ZnO and mulberry anthocyanin extract for active food packaging. *Food Hydrocolloids, 107,* 105942. https://doi.org/10.1016/j.foodhyd.2020.105942
23. Wang, H., Qian, J., Ding, F. (2018). Emerging chitosan-based films for food packaging applications. *Journal of Agricultural and Food Chemistry, 66(2),* 395–413. https://doi.org/10.1021/acs.jafc.7b04528
24. Gupta, M. S., Gowda, D. V., Kumar, T. P., Rosenholm, J. M. (2022). A comprehensive review of patented technologies to fabricate orodispersible films: Proof of patent analysis (2000–2020). *Pharmaceutics, 14(4),* 820. https://doi.org/10.3390/pharmaceutics14040820
25. Wang, H., Gong, X., Miao, Y., Guo, X., Liu, C. et al. (2019). Preparation and characterization of multilayer films composed of chitosan, sodium alginate and carboxymethyl chitosan-ZnO nanoparticles. *Food Chemistry, 283,* 397–403. https://doi.org/10.1016/j.foodchem.2019.01.022
26. Şenel, M., Ebru Koç, F. (2020). Controlled release of methylene blue from layer-by-layer assembled chitosan/polyacrylic acid. *International Journal of Polymeric Materials and Polymeric Biomaterials, 69(4),* 258–262. https://doi.org/10.1080/00914037.2018.1563082
27. Li, K., Zhu, J., Guan, G., Wu, H. (2019). Preparation of chitosan-sodium alginate films through layer-by-layer assembly and ferulic acid crosslinking: Film properties, characterization, and formation mechanism. *International Journal of Biological Macromolecules, 122,* 485–492. https://doi.org/10.1016/j.ijbiomac.2018.10.188
28. Zhang, W., Jiang, Q., Shen, J., Gao, P., Yu, D. et al. (2022). The role of organic acid structures in changes of physicochemical and antioxidant properties of crosslinked chitosan films. *Food Packaging and Shelf Life, 31,* 100792. https://doi.org/10.1016/j.fpsl.2021.100792

29. Babaee, M., Garavand, F., Rehman, A., Jafarazadeh, S., Amini, E. et al. (2022). Biodegradability, physical, mechanical and antimicrobial attributes of starch nanocomposites containing chitosan nanoparticles. *International Journal of Biological Macromolecules, 195,* 49–58. https://doi.org/10.1016/j.ijbiomac.2021.11.162
30. Du, Y., Yang, F., Yu, H., Yao, W., Xie, Y. (2022). Controllable fabrication of edible coatings to improve the match between barrier and fruits respiration through layer-by-layer assembly. *Food and Bioprocess Technology, 15(8),* 1778–1793. https://doi.org/10.1007/s11947-022-02848-7
31. Li, Y., Ying, Y., Zhou, Y., Ge, Y., Yuan, C. et al. (2019). A pH-indicating intelligent packaging composed of chitosan-purple potato extractions strength by surface-deacetylated chitin nanofibers. *International Journal of Biological Macromolecules, 127,* 376–384. https://doi.org/10.1016/j.ijbiomac.2019.01.060
32. Pismenskaya, N., Sarapulova, V., Klevtsova, A., Mikhaylin, S., Bazinet, L. (2020). Adsorption of anthocyanins by cation and anion exchange resins with aromatic and aliphatic polymer matrices. *International Journal of Molecular Sciences, 21(21),* 7874. https://doi.org/10.3390/ijms21217874
33. Yan, J., Zhang, H., Yuan, M., Qin, Y., Chen, H. (2022). Effects of anthocyanin-rich Kadsura coccinea extract on the physical, antioxidant, and pH-sensitive properties of biodegradable film. *Food Biophysics, 17(3),* 375–385. https://doi.org/10.1007/s11483-022-09727-w
34. Gasti, T., Dixit, S., D'souza, O. J., Hiremani, V. D., Vootla, S. K. et al. (2021). Smart biodegradable films based on chitosan/methylcellulose containing Phyllanthus reticulatus anthocyanin for monitoring the freshness of fish fillet. *International Journal of Biological Macromolecules, 187,* 451–461. https://doi.org/10.1016/j.ijbiomac.2021.07.128
35. Ezati, P., Tajik, H., Moradi, M. (2019). Fabrication and characterization of alizarin colorimetric indicator based on cellulose-chitosan to monitor the freshness of minced beef. *Sensors and Actuators, B: Chemical, 285,* 519–528. https://doi.org/10.1016/j.snb.2019.01.089
36. Fathi, M., Babaei, A., Rostami, H. (2022). Development and characterization of locust bean gum-Viola anthocyanin-graphene oxide ternary nanocomposite as an efficient pH indicator for food packaging application. *Food Packaging and Shelf Life, 34,* 100934. https://doi.org/10.1016/j.fpsl.2022.100934
37. Moalla, S., Ammar, I., Fauconnier, M. L., Danthine, S., Blecker, C. et al. (2021). Development and characterization of chitosan films carrying Artemisia campestris antioxidants for potential use as active food packaging materials. *International Journal of Biological Macromolecules, 183,* 254–266. https://doi.org/10.1016/j.ijbiomac.2021.04.113
38. Liu, J., Meng, C. G., Yan, Y. H., Shan, Y. N., Kan, J. et al. (2016). Protocatechuic acid grafted onto chitosan: Characterization and antioxidant activity. *International Journal of Biological Macromolecules, 89,* 518–526. https://doi.org/10.1016/j.ijbiomac.2016.04.089
39. Zhang, L., Liu, Z., Wang, X., Dong, S., Sun, Y. et al. (2019). The properties of chitosan/zein blend film and effect of film on quality of mushroom (Agaricus bisporus). *Postharvest Biology and Technology, 155,* 47–56. https://doi.org/10.1016/j.postharvbio.2019.05.013
40. Zeng, J., Ren, X., Zhu, S., Gao, Y. (2021). Fabrication and characterization of an economical active packaging film based on chitosan incorporated with pomegranate peel. *International Journal of Biological Macromolecules, 192,* 1160–1168. https://doi.org/10.1016/j.ijbiomac.2021.10.064
41. Butnaru, E., Stoleru, E., Brebu, M. A., Darie-Nita, R. N., Bargan, A. et al. (2019). Chitosan-based bionanocomposite films prepared by emulsion technique for food preservation. *Materials, 12(3),* 373. https://doi.org/10.3390/ma12030373
42. Savitri, E., Tjahayani, M. I., Say, A. A. N. (2022). Synthesis and characterization of chitosan-Allium sativum film. *AIP Conference Proceedings, 2470,* 040010 . https://doi.org/10.1063/5.0080203
43. Mohamed, N., Madian, N. G. (2020). Evaluation of the mechanical, physical and antimicrobial properties of chitosan thin films doped with greenly synthesized silver nanoparticles. *Materials Today Communications, 25,* 101372. https://doi.org/10.1016/j.mtcomm.2020.101372
44. Xu, J., Liu, K., Chang, W., Chiou, B. S., Chen, M. et al. (2022). Regulating the physicochemical properties of chitosan films through concentration and neutralization. *Foods, 11(11),* 1657. https://doi.org/10.3390/foods11111657

45. Liu, W., Xie, J., Li, L., Xue, B., Li, X. et al. (2021). Properties of phenolic acid-chitosan composite films and preservative effect on Penaeus vannamei. *Journal of Molecular Structure, 1239,* 130531. https://doi.org/10.1016/j.molstruc.2021.130531
46. Kaya, M., Ravikumar, P., Ilk, S., Mujtaba, M., Akyuz, L. et al. (2018). Production and characterization of chitosan based edible films from Berberis crataegina's fruit extract and seed oil. *Innovative Food Science and Emerging Technologies, 45,* 287–297. https://doi.org/10.1016/j.ifset.2017.11.013
47. Inthamat, P., Lee, Y. S., Boonsiriwit, A., Siripatrawan, U. (2022). Improving moisture barrier and functional properties of active film from genipin-crosslinked chitosan/astaxanthin film by heat curing. *International Journal of Food Science and Technology, 57(1),* 137–144. https://doi.org/10.1111/ijfs.15396
48. Yong, H., Wang, X., Bai, R., Miao, Z., Zhang, X. et al. (2019). Development of antioxidant and intelligent pH-sensing packaging films by incorporating purple-fleshed sweet potato extract into chitosan matrix. *Food Hydrocolloids, 90,* 216–224. https://doi.org/10.1016/j.foodhyd.2018.12.015
49. Roy, S., Rhim, J. W. (2021). Anthocyanin food colorant and its application in pH-responsive color change indicator films. *Critical Reviews in Food Science and Nutrition, 61(14),* 2297–2325. https://doi.org/10.1080/10408398.2020.1776211
50. Faroux, J. M., Borba, A., Ureta, M. M., Tymczyszyn, E. E., Gomez-Zavaglia, A. (2021). A combined approach of electronic spectroscopy and quantum chemical calculations to assess model membrane oxidation pathways. *New Journal of Chemistry, 45(44),* 20877–20886. https://doi.org/10.1039/d1nj03685h
51. Rachtanapun, P., Klunklin, W., Jantrawut, P., Jantanasakulwong, K., Phimolsiripol, Y. et al. (2021). Characterization of chitosan film incorporated with curcumin extract. *Polymers, 13(6),* 963. https://doi.org/10.3390/polym13060963
52. Wan, K., Cong, M., Teng, X., Feng, M., Ren, L. et al. (2021). Effects of pine bark extract on physicochemical properties and biological activity of active chitosan film by bionic structure of dragonfly wing. *Coatings, 11(9),* 012009. https://doi.org/10.3390/coatings11091077
53. Akalin, G. O., Oztuna Taner, O., Taner, T. (2022). The preparation, characterization and antibacterial properties of chitosan/pectin silver nanoparticle films. *Polymer Bulletin, 79(6),* 3495–3512. https://doi.org/10.1007/s00289-021-03667-0
54. Li, J., Zhuang, S. (2020). Antibacterial activity of chitosan and its derivatives and their interaction mechanism with bacteria: Current state and perspectives. *European Polymer Journal, 138,* 109984. https://doi.org/10.1016/j.eurpolymj.2020.109984
55. Ismillayli, N., Andayani, I. G. A. S., Honiar, R., Mariana, B., Sanjaya, R. K. et al. (2020). Polyelectrolyte complex (PEC) film based on chitosan as potential edible films and their antibacterial activity test. *IOP Conference Series: Materials Science and Engineering, 959(1),* 012009. https://doi.org/10.1088/1757-899X/959/1/012009
56. Wang, L., Liu, F., Jiang, Y., Chai, Z., Li, P. et al. (2011). Synergistic antimicrobial activities of natural essential oils with chitosan films. *Journal of Agricultural and Food Chemistry, 59(23),* 12411–12419. https://doi.org/10.1021/jf203165k
57. Chen, S., Zhang, Z., Wei, X., Sui, Z., Geng, J. et al. (2022). Antibacterial and antioxidant water-degradable food packaging chitosan film prepared from American cockroach. *Food Bioscience, 49,* 101893. https://doi.org/10.1016/j.fbio.2022.101893
58. Iqbal, M. H., Schroder, A., Kerdjoudj, H., Njel, C., Senger, B. et al. (2020). Effect of the buffer on the buildup and stability of tannic acid/collagen multilayer films applied as antibacterial coatings. *ACS Applied Materials and Interfaces, 12(20),* 22601–22612. https://doi.org/10.1021/acsami.0c04475
59. Cao, C., Kim, E., Liu, Y., Kang, M., Li, J. et al. (2018). Radical scavenging activities of biomimetic catechol-chitosan films. *Biomacromolecules, 19(8),* 3502–3514. https://doi.org/10.1021/acs.biomac.8b00809
60. Benbettaïeb, N., Tanner, C., Cayot, P., Karbowiak, T., Debeaufort, F. (2018). Impact of functional properties and release kinetics on antioxidant activity of biopolymer active films and coatings. *Food Chemistry, 242,* 369–377. https://doi.org/10.1016/j.foodchem.2017.09.065

61. Szymanowska, U., Baraniak, B. (2019). Antioxidant and potentially anti-inflammatory activity of anthocyanin fractions from pomace obtained from enzymatically treated raspberries. *Antioxidants, 8(8),* 299. https://doi.org/10.3390/antiox8080299
62. Dai, Q., Huang, X., Jia, R., Fang, Y., Qin, Z. (2022). Development of antibacterial film based on alginate fiber, and peanut red skin extract for food packaging. *Journal of Food Engineering, 330,* 111106. https://doi.org/10.1016/j.jfoodeng.2022.111106
63. Wang, X., Xie, Y., Ge, H., Chen, L., Wang, J. et al. (2018). Physical properties and antioxidant capacity of chitosan/epigallocatechin-3-gallate films reinforced with nano-bacterial cellulose. *Carbohydrate Polymers, 179,* 207–220. https://doi.org/10.1016/j.carbpol.2017.09.087
64. Prietto, L., Pinto, V. Z., El Halal, S. L. M., de Morais, M. G., Costa et al. (2018). Ultrafine fibers of zein and anthocyanins as natural pH indicator. *Journal of the Science of Food and Agriculture, 98(7),* 2735–2741. https://doi.org/10.1002/jsfa.8769
65. Luo, Q., Hossen, A., Sameen, D. E., Ahmed, S., Dai, J. et al. (2023). Recent advances in the fabrication of pH-sensitive indicators films and their application for food quality evaluation. *Critical Reviews in Food Science and Nutrition, 63(8),* 1102–1118. https://doi.org/10.1080/10408398.2021.1959296